

Ultrafast reversal of the ferroelectric polarization by a midinfrared pulse

Veniamin A. Abalmasov*

Institute of Automation and Electrometry SB RAS, 630090 Novosibirsk, Russia

(Dated: March 3, 2022)

We calculate the ferroelectric polarization dynamics induced by a femtosecond midinfrared pulse as measured in the recent experiment by R. Mankowsky et al., *Phys. Rev. Lett.* **118**, 197601 (2017). It is due to the nonlinear coupling of the excited infrared-active phonon with the ferroelectric mode or to the excitation of the ferroelectric mode itself depending on the pulse frequency. To begin with, we write the LiNbO₃ crystal symmetry invariant thermodynamic potential including electric field and nonlinear phonon coupling terms. We solve the equations of motion determined by this potential for phonon coordinates numerically in classical approximation. We explain the transient polarization reversal observed in the experiment by action of the depolarizing electric field which is due to bound charges at the polarization domain boundaries and give a reasonable estimate for its value. We argue that the polarization could be ultimately reversed when this field is screened.

INTRODUCTION

Control over polarization is essential for many applications of ferroelectrics, from non-volatile memory storing [1] to the switchable surface chemistry and catalysis [2]. The usual way of the polarization reversal by static or pulsed electric fields is limited in speed by hundreds of picoseconds [3]. Several proposals have been made how to switch the polarization on a time scale of picoseconds by directly exciting the ferroelectric mode with ultra-short radiation pulses [4–6]. However, they still have not been realized in practice. Though, a 90 degrees polarization rotation in a part of domains of a multi-domain ferroelectric thin film of (Ba_{0.8}Sr_{0.2})TiO₃ induced by a strong single-cycle terahertz pulse was claimed recently in [7]. At the same time, ultra-short (less than 20 ps) all-optical magnetic polarization control with low heat load in transparent ferromagnetic films has already been reported [8].

Recently, it has been proposed to switch the ferroelectric polarization by resonantly exciting infrared-active phonon mode nonlinearly coupled to the ferroelectric mode [9]. This approach, developed in last decades with an appearance of very high intensity lasers and called nonlinear phononics, has already proved to be successful in ultrafast lattice control [10]. The follow-up experiment [11] has indeed demonstrated a transient switching of the polarization in LiNbO₃ (LNO) crystal for laser pulse fluences larger than about 60 mJ/cm² (with the laser pulse duration of about 150 fs). One of possible explanations of the observed rapid polarization return to its initial state was the formation of uncompensated electric charges after polarization reversal in the irradiated part of the crystal [11] which has not been taken into account theoretically [4–6, 9, 11].

In this paper we calculate the phonon modes dynamics in conditions of the experiment [11]. We first argue that the equation of motion for the polarization is governed by the thermodynamic potential rather than a potential obtained from ab-initio calculations for the unrelaxed crystal which was used in [9, 11]. This implies that

nonlinear coupling terms must be invariant under symmetry transformations of the crystal parent group. We find biquadratic coupling constant values from the infrared phonons frequency shift at the ferroelectric phase transition which is known for LNO from ab-initio calculations. We solve numerically equations of motion for the coupled phonon modes and determine the depolarizing electric field value that corresponds better to the polarization dynamics observed in [11]. We propose to screen this field in experiment by a metallic wire deposited on the crystal surface around the irradiated spot in order to get an ultimate polarization reversal. We also show that an ultimate reversal of polarization in conditions of the experiment [11] is possible in our model when the ferroelectric mode is excited resonantly, though it demands very high pump fluences.

THEORETICAL APPROACH

In crystals, the movement of interacting with each other atoms near their equilibrium positions is a superposition of a complete set of normal modes $\{Q\}$ which are plain waves with definite frequencies and polarizations and which transform according to irreducible representations of the crystal symmetry group. According to the phenomenological Landau theory, the second order phase transition takes place when the coefficient of the quadratic term of one of the coordinates in the thermodynamic potential $F(\{Q\}, T)$ becomes negative below the critical temperature T_c . This leads to a non-zero thermal equilibrium value of this coordinate which is proportional to the spontaneous polarization in ferroelectrics [12].

It is believed that the thermodynamic potential determines the dynamics of the order parameter as well. In the case of a displacive structural phase transition the corresponding equation is [13]:

$$\ddot{Q} + \gamma\dot{Q} + \partial F(\{Q\}, T)/\partial Q = 0, \quad (1)$$

where γ is the damping constant. In the static case this

equation reduces to the usual thermal equilibrium condition. In the low-frequency range $F(\{Q\}, T)$ is calculated for fixed generalized forces conjugate to all other generalized coordinates. Thus understood Eq. (1), if valid up to optical phonon frequencies, expresses the essence of the so-called soft mode concept. Indeed, the square frequency in Eq. (1) is equal to the inverse static susceptibility $\chi^{-1}(T) = \partial^2 F(\{Q\}, T) / \partial Q^2$ which becomes zero at $T = T_c$. Only for high-frequency coordinates $F(\{Q\}, T)$ should be calculated for fixed values of the slowly changing coordinates [13].

We note that in [9] the potential $V(\{Q\})$ which determines equations of motion similar to Eq. (1) was calculated for PbTiO_3 crystal from first principles using density functional theory for fixed values (corresponding to the low-temperature ferroelectric phase) of all the rest of coordinates. For this reason the potential $V(\{Q\})$ was not symmetric in the ferroelectric mode coordinate Q_P (though the symmetry was restored when other coordinates were relaxed for a given value of Q_P) [9]. The thus obtained potential would be appropriate for a very fast dynamics of the ferroelectric mode. At the same time, in the experiment [11] the characteristic time change of Q_P is not smaller than its inverse frequency. Moreover, the signal of the second harmonics vanishes at some point. This implies that the crystal becomes centrosymmetric at this moment which is not possible when only the polarization vanishes but other coordinates are not relaxed with their values corresponding to the noncentrosymmetric ferroelectric phase.

LNO THERMODYNAMIC POTENTIAL

In what follows we will consider for concreteness the LNO crystal and the experiment scheme and conditions as in [11], see Fig. 1. Ferroelectric phase transition in LNO crystal occurs at the temperature about 1480 K from the paraelectric phase with symmetry $R\bar{3}c$ (D_{3d}^6) to the low-temperature ferroelectric phase with symmetry $R3c$ (C_{3v}^6) [14]. Two formula units in the unit cell implies 27 optical phonon modes, $4A_1 + 5A_2 + 9E$ in the ferroelectric phase and $A_{1g} + 2A_{1u} + 3A_{2g} + 3A_{2u} + 4E_g + 5E_u$ in the paraelectric phase. In the ferroelectric phase infrared-active polar optical phonon modes $A_1(\text{TO}_{1-4})$ have frequencies about 7.5, 8.1, 10 and 19 THz and $E(\text{TO}_{1-9})$ modes are with frequencies about 4.6, 7.0, 7.9, 9.7, 10.8, 11.1, 13.0, 17.3 and 19.8 THz [15, 16]. In the paraelectric phase $A_1(\text{TO}_3)$ has irreducible representation A_{1g} while the others are A_{2u} [14]. The mode $A_1(\text{TO}_1)$ becomes softer approaching the phase transition [17] and according to the first-principles calculations [18] it has the strongest overlap (0.82) with the mode A_{2u} which is unstable in the paraelectric phase and coincides with the atomic displacements during the phase transition. The mixing of $A_1(\text{TO}_1)$ and $A_1(\text{TO}_2)$ modes at temper-

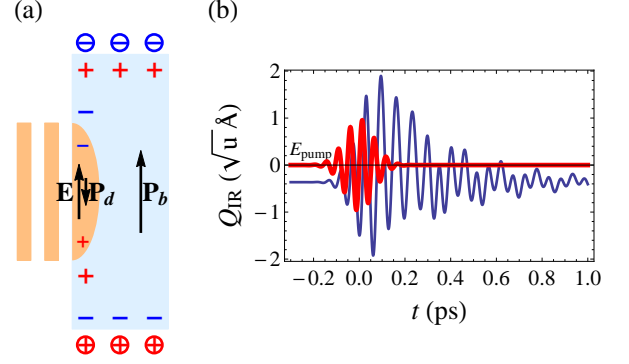


Figure 1. Sketch of the bulk and domain polarization $\mathbf{P}_{b,d}$ and electric field \mathbf{E} due to the bound charges in the sample when irradiated by a terahertz pulse; free charges on the surface are in circles (a) and the time-dependence of the terahertz radiation electric field (thick, red) and the corresponding infrared mode amplitude $Q_{A_1(\text{TO})_4}$ (blue) nonlinearly coupled to the ferroelectric mode at a fluence of 95 mJ/cm^2 (b).

atures between 400 and 600 K [17] is probably the cause of the incomplete overlap in the first-principles calculations. We will label the ferroelectric soft mode as Q_P and the other infrared-active modes Q_{IR} as $Q_{A_{1g}}$, $Q_{A_{2u}}$, $(Q_{E_g,x}, Q_{E_g,y})$ and $(Q_{E_u,x}, Q_{E_u,y})$ according to their irreducible representation.

During the ferroelectric phase transition the condensation of the soft mode occurs at the center of the Brillouin zone. The terahertz pulse as in the experiment [11] also excites mostly long-wavelength phonons. So we will consider an homogeneous case and neglect the interaction of phonons with different wavelengths coming from nonlinear phonon coupling.

The thermodynamic potential density $F(\{Q\}, T)$ that we want to write should be invariant under transformations of the parent paraelectric phase crystal symmetry group. We will write it as a sum

$$F = F_0 + F_{E\text{-ph}} + F_{\text{ph-ph}}. \quad (2)$$

The first part describes free phonons:

$$F_0 = -\frac{\omega_P^2}{4} Q_P^2 + \frac{c_P}{4} Q_P^4 + \frac{\omega_{\text{IR}}^2}{2} Q_{\text{IR}}^2, \quad (3)$$

where $\omega_{P,\text{IR}}$ are frequencies of the corresponding modes $Q_{P,\text{IR}}$. The coefficient c_P determines the equilibrium value Q_P^e through the equation $\partial F / \partial Q_P = 0$. In the absence of electric field and nonlinear phonon interactions this gives $c_P = \omega_P^2 / (2(Q_P^e)^2)$. Summation over all infrared-active modes Q_{IR} in Eq. (3) is assumed.

As a function of the ferroelectric mode amplitude $F_0(Q_P)$ was calculated ab-initio, for instance, in [19] and when fitted to a forth order polynomial it provided the energy difference between the ground and the lowest excited state in agreement with experimental data.

The second part of the thermodynamic potential corresponds to the phonon-electric field coupling:

$$F_{E\text{-ph}} = -E_z(Z_P^*Q_P + Z_{A_{2u}}^*Q_{A_{2u}} + Z_{A_{1g}}Q_PQ_{A_{1g}}) - \sum_{j=x,y} E_j(Z_{E_u}^*Q_{E_u,j} + Z_{E_g}Q_PQ_{E_g,j}), \quad (4)$$

where $Z_{P,\text{IR}}^*$ are Born effective charges of the corresponding modes $Q_{P,\text{IR}}$, Z_{A_{1g},E_g} are coupling constants, $E_{x,y,z}$ are the electric field components.

We see from Eq. (4) that coupling of the electric field to symmetric phonon modes A_{1g} and E_g is possible only in ferroelectric phase, when $\langle Q_P \rangle \neq 0$. Though, even in ferroelectric phase this coupling is expected to be not large due to the small value of $\langle Q_P \rangle$. Indeed, the effective charge of $A_1(\text{TO}_3)$, which has irreducible representation A_{1g} in paraelectric phase, is very small [15].

We will focus on a single phonon mode excitation and as a consequence only on two-phonon modes coupling, one of each is the ferroelectric soft mode Q_P and the other is an infrared-active mode Q_{IR} (see [20, 21] for discussions on three phonon modes interaction). The leading coupling terms in phonon amplitudes (up to the forth order) are

$$F_{\text{ph-ph}} = \sum_{i=1,2} a_i Q_P^2 Q_{A_{1g}}^i + \sum_{i=1,2,3} c_i Q_P^i Q_{A_{2u}}^{4-i} + \sum_{\substack{i=g,u \\ j=x,y}} b_i Q_P^2 Q_{E_{i,j}}^2 + d Q_P Q_{E_{u,y}} (3Q_{E_{u,x}}^2 - Q_{E_{u,y}}^2). \quad (5)$$

Three-phonons interaction in Eq. (5) with the coupling constant a_1 is not of much interest to us because it is difficult to excite A_{1g} mode as we discussed above (since its effective charge is proportional to Q_P , this term effectively is of the forth order in phonon coordinates).

In what follows we apply the thermodynamic potential (2) through Eq. (1) to describe the results of the experiment [11] where the mode $A_1(\text{TO}_4)$ was pumped resonantly by a high-intensity femtosecond electromagnetic pulse. For this purpose we precise in the next section the numerical values of parameters which enter Eqs. (1) - (2).

VALUES OF PARAMETERS

The electric field in Eq. (4) has two constituents, $E_z = E_1 + E_2$, the both being directed along z -axis in the experiment [11]. One is the driving midinfrared pulse electric field $E_1(t) = E_0 \sin(\omega t) \exp(-4 \ln 2 t^2/T^2)$ with frequency ω , Gaussian envelope of duration $T = 0.15$ ps and amplitude E_0 up to 25 MV/cm in the experiment [11], see Fig. 1(b). The other component is due to the depolarizing electric field E_d in the reversed polarization domain created by the terahertz pump (Fig. 1(a)). We suppose there is no screening of this field by free carriers on the time scale of the polarization reversal

as in the experiment [11]. So the resulting field is $E_2(t) = E_d(1 - Q_P(t)/Q_P^e)$.

We calculate the effective electric charge of a given optical mode from the experimental value of its oscillation strength [22]. Thus, we obtain $Z_P^* = 1.356$, $Z_{A_1(\text{TO}_2)}^* = 0.564$ and $Z_{A_1(\text{TO}_4)}^* = 1.404 e/\sqrt{u}$. The effective charge $Z_{A_1(\text{TO}_3)}^*$ is very small [17] and we will neglect the dynamics of this mode.

The ions shifts between paraelectric and ferroelectric phase at room temperature according to [23] correspond to $Q_P^e = 2.9\sqrt{u}\text{\AA}$ which agrees with the minimum position of the two-minimum energy surface calculated in [19]. At the same time, according to the experimental data [24] the Li and O atoms are shifted in the ferroelectric phase by about $\Delta z_{\text{Li}} = 0.460 \text{\AA}$ and $\Delta z_{\text{O}} = 0.270 \text{\AA}$ which gives the amplitude $Q_P^e = (\sum_i m_i \Delta z_i^2)^{1/2} = 3.1\sqrt{u}\text{\AA}$. The same value of Q_P^e , which we adopt in our calculations, follows from atomic displacements calculated ab-initio [14, 18, 25]. Q_P^e enters Eq. (1) as an initial value of the $Q_P(t)$ coordinate. Initial values of other coordinates are obtained from the equilibrium condition $\partial F/\partial Q_{\text{IR}} = 0$ and they are not zero when the modes are nonlinearly coupled, see Fig. 1(b). This also can explain a partial overlap of ferroelectric soft modes in para- and ferroelectric phases as it was discussed above.

We note that the spontaneous polarization $P_s = Z_P^* Q_P^e/v_0$, v_0 being the unit cell volume, calculated for $Q_P^e = 3.1\sqrt{u}\text{\AA}$ is about 0.64 C/m^2 and slightly lower than the experimental value about $P_s = 0.70 \text{ C/m}^2$ [18] which in its turn is attained for a rather large value $Q_P^e = 3.4\sqrt{u}\text{\AA}$. This slight discrepancy can also be attributed to the highly nonlinear evolution of the charges along the ferroelectric path of atomic displacements [18].

We adopt the values for the damping constants in Eq. (1) from [22] to be $\tilde{\gamma}_P = 0.8$, $\tilde{\gamma}_{A_1(\text{TO}_2)} = 0.6$ and $\tilde{\gamma}_{A_1(\text{TO}_4)} = 1.0 \text{ THz}$ (with $\gamma = 2\pi\tilde{\gamma}$). The damping $\tilde{\gamma}_P$ increases strongly with temperature and equals the soft mode frequency of 5 THz at about 1100 K [17]. It is not clear whether this is due to the mode softening or just to the temperature dependence. We keep the damping $\tilde{\gamma}_P$ constant in our calculations.

Finally, we note that the biquadratic phonon-phonon interaction with the coupling constant c_2 in Eq. (5) does change not only the frequency of the soft mode Q_P but the frequency of the Q_{IR} as well, Eq. (3). This allows, for instance, in some cases to reproduce the polarization temperature dependence from high-frequency modes temperature dependence [26, 27]. Usually the effect is not large. For the ferroelectric KDP crystal, however, the change is about ten percent for certain modes indicating both signs of the coupling constant [28, 29]. So we calculate the coupling constant as $c_2 = (\omega_{\text{IR}}^2 - \Omega_{\text{IR}}^2)/2(Q_P^e)^2$ where ω_{IR} and Ω_{IR} are the frequencies of the Q_{IR} mode in the ferroelectric and paraelectric phases respectively, Q_P^e is the thermal equilibrium value of Q_P at room temperature. The positive sign of the coupling constant assures

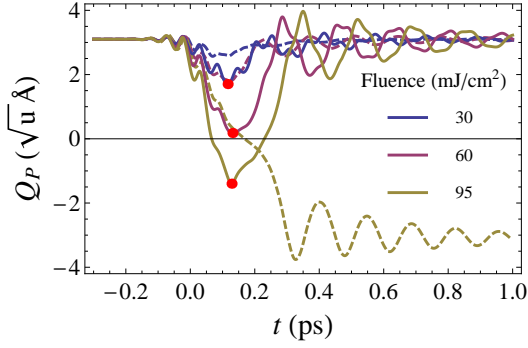


Figure 2. Ferroelectric mode dynamics for the pump pulse fluences of 30, 60 and 95 mJ/cm² and frequency $\omega = 19$ THz when $c_{1,3} = 0$ and $E_d = 0$ (dashed) and $c_1 = 10$, $c_3 = 17$ meV/u²Å⁴ for $A_1(\text{TO}_4)$ and $E_d = 2.8$ MV/cm (solid). Red dots are at minimums of Q_P

a single well potential $F(Q_P)$ for large values of Q_{IR}^2 and thus a possibility of the polarization reversal. We note that ω_{IR} does not change substantially in the ferroelectric phase of LNO up to about 1000 K [17, 30] but this agrees with a small change in the polarization itself in this temperature range [31].

Due to the very high temperature of the phase transition the values of Ω_{IR} for LNO crystal are available only from first-principles calculations. For $A_1(\text{TO}_4)$ they vary from 15.6 [14] and 14.3 [18] to 13.6 THz [25], for $A_1(\text{TO}_2)$ from 3.5 [14] and 2.8 [18] down to 0.9 THz [25]. For $A_1(\text{TO}_3)$ in contrast the frequency is larger in the paraelectric phase varying from 12.1 [14, 18] to 10 THz [25] which indicates a possible negative value of the bi-quadratic phonon-phonon coupling constant. We adopt values $\Omega_{A_1(\text{TO}_4)} = 14$ THz and $\Omega_{A_1(\text{TO}_2)} = 3.5$ THz which correspond to $c_{2,A_1(\text{TO}_4)} = 34$ meV/u²Å⁴ and $c_{2,A_1(\text{TO}_2)} = 11$ meV/u²Å⁴. We note that our coupling constants appear to be an order of magnitude smaller than those obtained for quantum paraelectric crystals KTaO_3 [32] and SrTiO_3 [33] from DFT calculations. This might be due to the calculation procedure of the potential discussed in Sec. . Indeed, a relaxed lattice has the lowest energy and, as a consequence, the nonlinear phonon coupling constants of our thermodynamic potential are smaller.

We keep coupling constants c_1 and c_3 in Eq. (5) and the depolarizing electric field E_d in Eq. (4) as fitting parameters in our calculations when compared to the experimental results [11].

CALCULATION RESULTS

We start with zero values of coupling constants $c_{1,3}$ and the depolarizing electric field E_d and calculate the phonon modes dynamics for three values of the infrared pulse fluence, see Fig. 2. In the experiment [11] for flu-

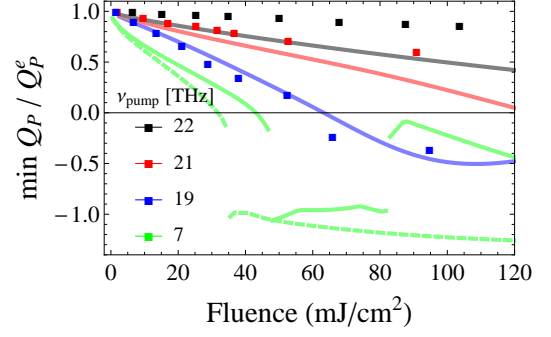


Figure 3. Minimum of Q_P (normalized by Q_P^e) as a function of fluence for different frequencies of the pump pulse. At $\nu_{\text{pump}} = 7$ THz two lines correspond to opposite signs of the pump pulse electric field. Experimental data are from [11]

ences above a threshold value of 60 mJ/cm² the second-harmonic intensity (and thus the ferroelectric mode Q_P) was observed to vanish completely. We see, however, only a reduction of it at this fluence. The dynamics becomes closer to the experiment if we put $c_{2,A_1(\text{TO}_4)} = 51$ meV/u²Å⁴ but this corresponds to the very low frequency $\Omega_{A_1(\text{TO}_4)} = 10.7$ THz expected in paraelectric phase. Interestingly, the situation can be improved if we take a positive value of the constant $c_{3,A_1(\text{TO}_4)} \gtrsim 13$ meV/u²Å⁴. It is rather unexpected because the force exerted by this coupling on Q_P oscillates and changes its sign. At the same time, negative values of $c_{3,A_1(\text{TO}_4)}$ make the polarization reversal even harder. Finite values of $c_{1,A_1(\text{TO}_4)}$ do not influence much the dynamics. This can be easily understood because the latter coupling is cubic in Q_{IR} while the former is linear and $Q_{\text{IR}} \ll Q_P$.

The reentrant behavior of the polarization for the largest fluence of 95 mJ/cm² available in [11] appears for depolarizing electric fields larger than about $E_d \approx 2.5$ MV/cm. This value to be compared with the depolarizing field in a plate-like monodomain sample $E_d = P_s/(\epsilon\epsilon_0)$ which is about 26.4 MV/cm for $P_s = 0.70$ C/m² and the dielectric constant $\epsilon_{33} = 30$ in LNO (ϵ_0 is the electric constant). The value of the depolarization factor $N \approx 0.1$ seems to be reasonable taken into account the oblong shape of the reversed polarization domain created (the pump penetration depth is about 3.2 μm [11] and its spot size is about 65 μm [22], see Fig. 1(a)).

Finally, we adopt the values $E_d = 2.8$ MV/cm and $c_1 = 10$ and $c_3 = 17$ meV/u²Å⁴ for $A_1(\text{TO}_4)$ mode, see Fig. 2. For $A_1(\text{TO}_2)$ we keep these coupling constants zero since its dynamics (due to the small Born electric charge $Z_{A_1(\text{TO}_2)}^*$) does not influence visibly the dynamics of Q_P even near the resonance which is close to the resonance of Q_P itself.

We calculate the minimum value of Q_P (normalized by Q_P^e) as a function of fluence for different frequencies of the pump pulse (with the same Gaussian envelope duration) and compare our results to the experiment [11],

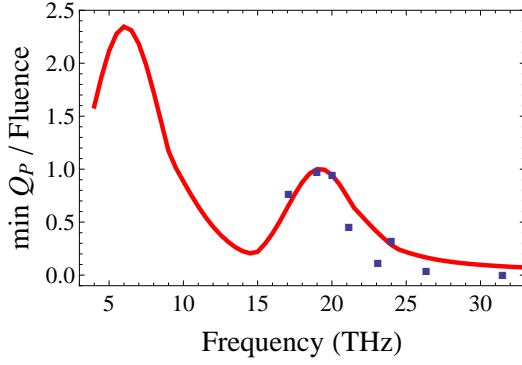


Figure 4. Susceptibility as a function of the pump frequency normalized to unity at 19 THz. Experimental data are from [11]

see Fig. 3. The agreement is good enough. For the pump frequency of 7 THz, which is close to the ferroelectric mode resonance, the result depends slightly on the sign (phase) of the pulse oscillations due to comparable values of the pump duration and the period of oscillations. For this pump frequency we see an ultimate reversal of the polarization for fluences higher than about 40 mJ/cm². The reversal becomes even harder for larger values of the depolarizing field until it becomes impossible if $E_d \gtrsim 5$ MV/cm. This threshold corresponds to the coercive field value in our model, $E_c = P_s / (3\sqrt{3}\epsilon\epsilon_0)$ in the absence of electric field and nonlinear phonons coupling, at which the metastable state (local minimum) with opposite polarization disappears. We note, however, that it is an order of magnitude larger than experimental values of the coercive field in this crystal [34].

The dependence of the susceptibility $\min Q_P$ /fluence calculated for small fluences as a function of the pump frequency reproduces the experimental results [11] as well (Fig. 4). The width of peaks is determined mostly by the frequency width of the pump pulse.

DISCUSSION

In our calculations we see the oscillations of Q_P with the ferroelectric mode frequency which are absent in the experiment [11]. In the experiment these oscillations could be smeared for several reasons. First, initial values of velocities are not zero and those of coordinates are not at equilibrium but they are determined instead by the temperature and the coordinates wave functions. Second, the electric field amplitude of the midinfrared pulse which penetrates the crystal is not homogeneous and is determined by the Gaussian function perpendicular to its direction and a vanishing exponential deep into the crystal, $\exp(-z/z_0)$ with $z_0 \approx 3.5 \mu\text{m}$, while the second harmonic is generated at $z \lesssim 1 \mu\text{m}$ [11]. Finally, the nonlinear coupling to the phonon modes with nonzero wave

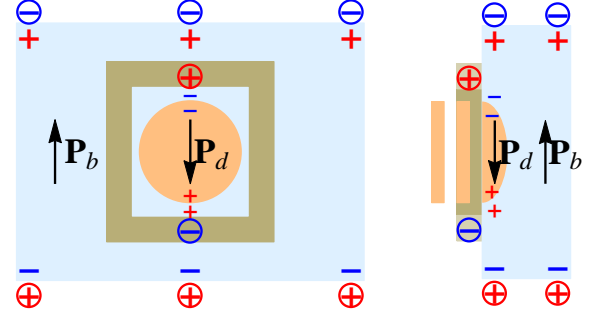


Figure 5. Sketch of the screen (in golden) on the top of the crystal around the pump laser spot and the electric charges distribution (free charges are in circles)

numbers which we have not taken into account would probably also lead to the polarization oscillations smearing.

High-intensity sources of far-infrared electromagnetic fields (more than 3.5 MV/cm) tunable between 4 and 18 THz were reported recently in [35]. These fluences, however, are not high enough to switch the polarization by the resonant pump of the ferroelectric mode (Fig. 3). A very high-intensity source of terahertz single-cycle pulse (up to 22 MV/cm) was reported in [36] but its frequency is about 1 THz only. Thus, the resonant ferroelectric mode reversal in LNO seems to be unattainable at the moment.

Our calculations show, however, that the polarization can be ultimately switched in the absence of the depolarizing field (Fig. 2). In order to screen this field a metallic wire could be used which is drawn in golden in Fig. 5. The relaxation time of this screen $\tau = RC$ is determined by the resistance $R \approx \rho L / (h + d)\delta$ and capacitance $C \approx \epsilon\epsilon_0 h$ of the wire. The resistivity and skin depth for gold at frequency 10 THz are $\rho \sim 10^{-7} \Omega \text{ m}$ and $\delta \approx 30 \text{ nm}$. The metallic wire length, height and width are about $L \approx 400 \mu\text{m}$, $h \sim d \sim 10 \div 100 \mu\text{m}$. This yields the relaxation time smaller than $\tau \sim 0.1 \text{ ps}$, which is enough to follow the polarization dynamics (Fig. 2).

Recently, anharmonic oscillations of the lowest frequency E mode in LNO were studied under resonant excitation by a single-cycle pulse with the electric field about 1 MV/cm [37]. At the same time, it would be interesting to see the dynamics of the ferroelectric mode Q_P induced by the resonant excitation of the E modes, Eqs. (4)-(5), due to their nonlinear coupling as it was described in this work for the A modes excitation, especially keeping in mind orthogonal polarizations of the A and E modes. Calculated ab-initio E modes frequencies [14, 25] differ substantially in para- and ferroelectric phases meaning possible strong coupling constants of these modes to the ferroelectric mode.

CONCLUSION

Our calculations of the ferroelectric mode dynamics in LNO, determined by the parent phase symmetry-invariant thermodynamic potential, reproduce well the transient reversal of polarization under high-frequency mode excitation reported in [11] when the electric field of the bound charges is taken into account. The estimated strength of this field agrees with the polarization value in LNO and the expected depolarization factor of the transiently created polarization domain. We argue that the polarization could be ultimately reversed if the depolarizing field is screened, for example by the metallic wire on the top of the crystal around the pump laser spot. We preview that the same dynamics of the polarization could be probed by the resonant excitation of the E modes which are orthogonal to the polarization.

ACKNOWLEDGMENTS

I thank Roman Mankowsky and Alaska Subedi for useful discussions.

The study was carried out with the financial support of the Russian Foundation for Basic Research in the framework of the scientific project No. 18-02-00399.

* abalmasov@iae.nsc.ru

- [1] J. F. Scott, Applications of modern ferroelectrics, *Science* **315**, 954 (2007).
- [2] A. Kakekhani, S. Ismail-Beigi, and E. I. Altman, Ferroelectrics: A pathway to switchable surface chemistry and catalysis, *Surface Science* **650**, 302 (2016).
- [3] J. Li, B. Nagaraj, H. Liang, W. Cao, C. H. Lee, and R. Ramesh, Ultrafast polarization switching in thin-film ferroelectrics, *Applied Physics Letters* **84**, 1174 (2004).
- [4] S. Fahy and R. Merlin, Reversal of ferroelectric domains by ultrashort optical pulses, *Phys. Rev. Lett.* **73**, 1122 (1994).
- [5] T. Qi, Y.-H. Shin, K.-L. Yeh, K. A. Nelson, and A. M. Rappe, Collective Coherent Control: Synchronization of Polarization in Ferroelectric PbTiO_3 by Shaped THz Fields, *Phys. Rev. Lett.* **102**, 247603 (2009).
- [6] R. Herchig, C.-M. Chang, B. K. Mani, and I. Ponomareva, An unusual route to polarization reversal in ferroelectric ultrathin nanowires, *Applied Physics Letters* **105**, 012907 (2014).
- [7] K. A. Grishunin, N. A. Ilyin, N. E. Sherstyuk, E. D. Mishina, A. Kimel, V. M. Mukhortov, A. V. Ovchinnikov, O. V. Chefonov, and M. B. Agranat, THz electric field-induced second harmonic generation in inorganic ferroelectric, *Scientific Reports* **7**, 687 (2017).
- [8] A. Stupakiewicz, K. Szerenos, D. Afanasiev, A. Kirilyuk, and A. V. Kimel, Ultrafast nonthermal photomagnetic recording in a transparent medium, *Nature* **542**, 71 (2017).
- [9] A. Subedi, Proposal for ultrafast switching of ferroelectrics using midinfrared pulses, *Phys. Rev. B* **92**, 214303 (2015).
- [10] M. Först, C. Manzoni, S. Kaiser, Y. Tomioka, Y. Tokura, R. Merlin, and A. Cavalleri, Nonlinear phononics as an ultrafast route to lattice control, *Nature Physics* **7**, 854 (2011).
- [11] R. Mankowsky, A. von Hoegen, M. Först, and A. Cavalleri, Ultrafast reversal of the ferroelectric polarization, *Phys. Rev. Lett.* **118**, 197601 (2017).
- [12] L. Landau and E. Lifshitz, *Course of Theoretical Physics*, 3rd ed., Vol. 5 (Elsevier Science, 2013).
- [13] V. Ginzburg, A. Levanyuk, and A. Sobyannin, Light scattering near phase transition points in solids, *Physics Reports* **57**, 151 (1980).
- [14] K. Parlinski, Z. Q. Li, and Y. Kawazoe, Ab initio calculations of phonons in LiNbO_3 , *Phys. Rev. B* **61**, 272 (2000).
- [15] S. Kojima, K. Kanehara, T. Hoshina, and T. Tsurumi, Optical phonons and polariton dispersions of congruent LiNbO_3 studied by far-infrared spectroscopic ellipsometry and Raman scattering, *Japanese Journal of Applied Physics* **55**, 10TC02 (2016).
- [16] S. Margueron, A. Bartasyte, A. M. Glazer, E. Simon, J. Hlinka, I. Gregora, and J. Gleize, Resolved E-symmetry zone-centre phonons in LiTaO_3 and LiNbO_3 , *Journal of Applied Physics* **111**, 104105 (2012).
- [17] A. Ridah, M. D. Fontana, and P. Bourson, Temperature dependence of the Raman modes in LiNbO_3 and mechanism of the phase transition, *Phys. Rev. B* **56**, 5967 (1997).
- [18] M. Veithen and P. Ghosez, First-principles study of the dielectric and dynamical properties of lithium niobate, *Phys. Rev. B* **65**, 214302 (2002).
- [19] I. Inbar and R. E. Cohen, Origin of ferroelectricity in LiTaO_3 and LiNbO_3 ; LAPW total energy calculations, *Ferroelectrics* **164**, 45 (1995).
- [20] D. M. Juraschek, M. Fechner, and N. A. Spaldin, Ultrafast structure switching through nonlinear phononics, *Physical Review Letters* **118**, 054101 (2017).
- [21] P. G. Radaelli, Breaking symmetry with light: Ultrafast ferroelectricity and magnetism from three-phonon coupling, *Phys. Rev. B* **97**, 085145 (2018).
- [22] A. von Hoegen, R. Mankowsky, M. Fechner, M. Först, and A. Cavalleri, Probing the interatomic potential of solids with strong-field nonlinear phononics, *Nature* **555**, 79 (2018).
- [23] M. Lines and A. Glass, *Principles and Applications of Ferroelectrics and Related Materials*, International series of monographs on physics (OUP Oxford, 2001).
- [24] H. Boysen and F. Altorfer, A neutron powder investigation of the high-temperature structure and phase transition in LiNbO_3 , *Acta Crystallographica Section B* **50**, 405 (1994).
- [25] M. Friedrich, A. Riefer, S. Sanna, W. G. Schmidt, and A. Schindlmayr, Phonon dispersion and zero-point renormalization of LiNbO_3 from density-functional perturbation theory, *Journal of Physics: Condensed Matter* **27**, 385402 (2015).
- [26] A. S. Krylov, A. N. Vtyurin, A. S. Oreshonkov, V. N. Voronov, and S. N. Krylova, Structural transformations in a single-crystal Rb_2NaYF_6 : Raman scattering study,

- [Journal of Raman Spectroscopy](#) **44**, 763 (2013).
- [27] E. K. H. Salje and U. Bismayer, Hard mode spectroscopy: The concept and applications, [Phase Transitions](#) **63**, 1 (1997).
 - [28] F. Brehat and B. Wyncke, Low-frequency models in KH_2PO_4 -type crystals, [International Journal of Infrared and Millimeter Waves](#) **8**, 155 (1987).
 - [29] P. Simon, F. Gervais, and E. Courtens, Paraelectric-ferroelectric phase transitions of KH_2PO_4 , RbH_2PO_4 , and KH_2AsO_4 studied by infrared reflectivity, [Phys. Rev. B](#) **37**, 1969 (1988).
 - [30] W. D. Johnston and I. P. Kaminow, Temperature Dependence of Raman and Rayleigh Scattering in LiNbO_3 and LiTaO_3 , [Phys. Rev.](#) **168**, 1045 (1968).
 - [31] R. I. Shostak, S. V. Yevdokimov, and A. V. Yatsenko, An analysis of the temperature dependence of the spontaneous polarization of LiNbO_3 crystals, [Crystallography Reports](#) **54**, 492 (2009).
 - [32] A. Subedi, Midinfrared-light-induced ferroelectricity in oxide paraelectrics via nonlinear phononics, [Physical Review B](#) **95**, 134113 (2017).
 - [33] M. Kozina, M. Fechner, P. Marsik, T. van Driel, J. M. Glowacki, C. Bernhard, M. Radovic, D. Zhu, S. Bonetti, U. Staub, and M. C. Hoffmann, Terahertz-driven phonon upconversion in SrTiO_3 , [Nature Physics](#) **15**, 387 (2019).
 - [34] T. Volk and M. Wöhlecke, [Lithium Niobate](#) (Springer Berlin Heidelberg, 2008).
 - [35] B. Liu, H. Bromberger, A. Cartella, T. Gebert, M. Först, and A. Cavalleri, Generation of narrowband, high-intensity, carrier-envelope phase-stable pulses tunable between 4 and 18 THz, [Optics Letters](#) **42**, 129 (2017).
 - [36] A. V. Ovchinnikov, O. V. Chefonov, E. D. Mishina, and M. B. Agranat, Second harmonic generation in the bulk of silicon induced by an electric field of a high power terahertz pulse, [Scientific Reports](#) **9**, 9753 (2019).
 - [37] B. S. Dastrup, J. R. Hall, and J. A. Johnson, Experimental determination of the interatomic potential in LiNbO_3 via ultrafast lattice control, [Applied Physics Letters](#) **110**, 162901 (2017).